

A new chaotic network model for epilepsy

Shirin Panahi^a, Touraj Shirzadian^{b,c}, Mahdi Jalili^d, Sajad Jafari^{a,*}



^a Biomedical Engineering Department, Amirkabir University of Technology, Tehran 15875-4413, Iran

^b Department of Biotechnology, Faculty of New Sciences and Technologies, Semnan University, Semnan, Iran

^c Kermanshah University of Medical Sciences, Kermanshah, Iran

^d School of Engineering, RMIT University, Melbourne, Australia

ARTICLE INFO

Keywords:

Analytical modeling
Epilepsy
Seizure
Chaotic behavior
Neural network

ABSTRACT

Epilepsy is a prevalent neurological disorder with symptoms characterized by abnormal discharge in the brain. According to the classification of the International League Against Epilepsy (ILAE) Commission, temporal lobe epilepsy is the most common type of epilepsy accounting for the most cases of the disorder observed in patients. Electroencephalography (EEG) is the most common diagnostic tool for Epilepsy, by which abnormal electrical activity of the brain can be clearly seen. This paper uses chaos theory and proposes a new analytical mass model for temporal lobe Epilepsy. Chaotic behavior of the model indicates normal model, while its periodic behavior indicate epileptic mode of the brain. The proposed model includes a number of parameters for which a full bifurcation analysis is conducted. This fully characterizes different regimes of the model and allows studying how one can control the parameters to switch between different modes. The proposed model enables to effectively use advance chaos-based mathematical tools to get further insights on the underlying mechanisms of epilepsy.

© 2018 Elsevier Inc. All rights reserved.

1. Introduction

Epilepsy is known to be a series of seizures which is a transient incidence of some signs and/or symptoms. These seizures may occur as a result of malformed synchronous and excessive neural brain activities. It is the second most common disease of the nervous system after stroke affecting almost 1% of people worldwide [1–3]. Among all kinds of seizure, temporal lobe Epilepsy is the most common type of the disease accounting for around 30–35% of the cases [4–6]. It is thus necessary to expand research studies on epilepsy, understand its basic initiation mechanisms and find a better way for therapy and control. One of common techniques in many theoretical studies is computational modeling, which provides a proper insight on understanding the pathological behavior of neural networks. Furthermore, computational modeling combined with real data can indeed create a virtual laboratory for testing the new therapeutic approaches before clinical trials.

The brain is a complex system producing highly nonlinear behavior and there are many recent studies using nonlinear dynamics as a tool for brain functional modeling [10–17]. There are also recent results showing that many biological systems show chaotic behavior. For example, a research by Crevier et al. showed that response of human and salamander retina to the flicker of light may be chaotic [18,19]. Freeman et al. claimed existence of chaotic behavior in the brain by studying the brain function in healthy and epileptic rats. By the invention of Electroencephalogram (EEG) in the early 19th century and the advent of recording the electrical activity of the brain from the skull, discovering hidden patterns of EEG-based

* Corresponding author.

E-mail addresses: sajadjafari@aut.ac.ir, sajadjafari83@gmail.com (S. Jafari).

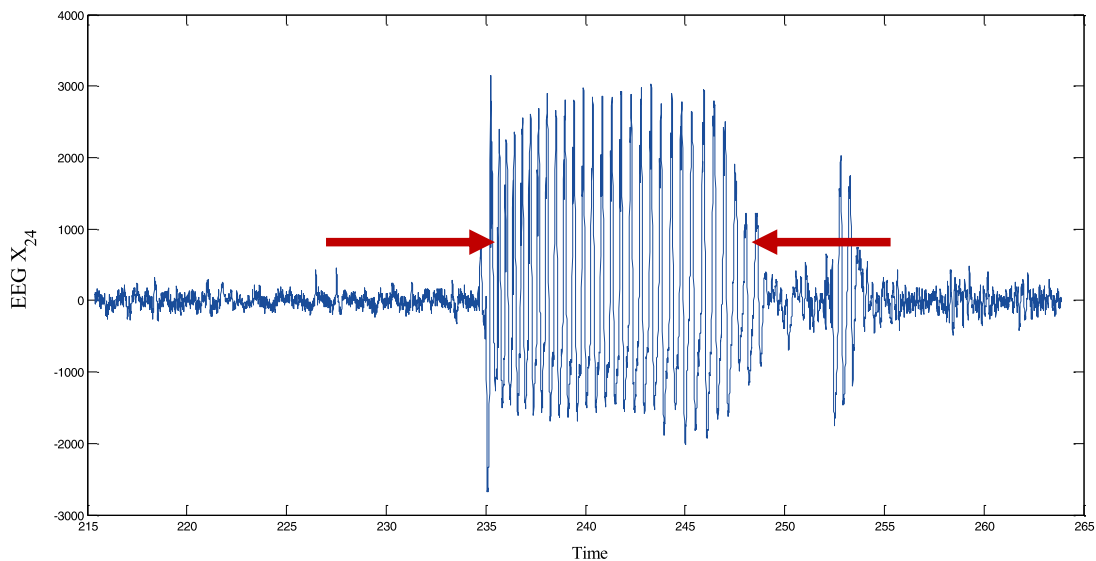


Fig. 1. An example of EEG signal recorded during a seizure [48].

brain signals is a common practice for many brain disorders [7]. The different behavior seen in the EEG signal is not only sensible but affected by the changes in the brain's different parameters [8]. Such behavior makes these systems similar in some aspects to chaotic systems [9]. Brain is a dynamical system producing behaviors that are not fixed at any point, but often switching between different modes. For example, a brain disease might switch its behavior from normal (chaotic) to a harmonious state (periodic), like what often observed in attention deficit disorder [10] or an epileptic seizure [11]. These changes in the dynamics of a system are known as a bifurcation [12]. The occurrence of a seizure can be interpreted as a bifurcation as the normal brain function suddenly changes to an abnormal behavior [13–16].

Synchronization can occur in a network of chaotic systems [17–19]. It is responsible for many phenomena like spiral waves and chimera states [20–26]. Periodic window in chaotic systems is the phenomenon seen in bifurcation diagrams, in which the overall behavior of the system changes from chaotic to periodic. The system might change its behavior back to chaotic if one keeps changing this parameter. In a similar way, seizure disrupts the normal functioning of the brain (from chaotic behavior) for a while after which the nervous system returns to the normal function when seizures end. Modeling studies of the nervous system can be generally divided into three categories as follows. (i) *Detailed neuronal models*: These models try to explain some details about biological mechanisms such as current flows in the membrane ion channels. With these models, researchers can study a number of behaviors of the epileptic dynamic cell [27,28]. (ii) *Neural mass models*: These are more abstract models studying the dynamics of a population of nerve cells in the network. These models do not have any attention to the details of one cell [29–37]. (iii) *Analytical models*: These models only try to describe the general behavior of the system in mathematical terms. All details about cells, populations, or connections are often ignored, however essential general dynamics of the system, such as system states and transitions between the states, are conserved [38]. In this study, an interstitial approach is proposed to model epilepsy as a chaotic system. The proposed model allows an analytical approach to study the temporal lobe epilepsy taking into account physiological facts.

The rest of the paper is organized as follows. Section 2 is a comprehensive physiological background about epilepsy. The computational model of the brain activity in normal and disorder moods is proposed in Section 3, and properties of the proposed model supported by numerical simulations is presented in Section 4. Finally, the paper is concluded in Section 5.

2. The physiological background

Epilepsy is a prevalent neurological disorder/or symptoms characterized by abnormal discharges in the brain. There are many types of epilepsy but according to the International League Against Epilepsy (ILAE) Commission, the seizures are classified into two main categories: partial (focal or local) and generalized seizure. Among them, temporal lobe epilepsy is the most common type of the disease [4–6]. It belongs to the category of partial seizure which initiates from one part in the temporal lobe (that is also known as foci) and propagates to only one part of the brain. In addition to its prevalence, it is mostly resistant to treatment which causes more concern and sensitivity.

The cause of epileptic seizures is unclear in more than 60% of the cases [39,40]. One of the main reasons, among the known causes may be a reinforcing coordinated activity of many local neurons in a state of high excitability [41,42]. Generally, this situation includes the abnormal interaction between inhibition GABAergic and excitatory Glutamatergic mechanisms [43,44]. Meanwhile, aberrant dynamics of neural networks play an important role in emergence of the seizures [45]. The central nervous system is a complex network of various cell types connected to each other via synapses, electric and/or

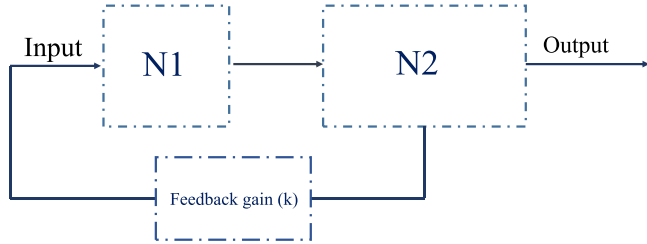


Fig. 2. The schematic of proposed model which contains two main parts, N_1 and N_2 with a feedback, representing different portions of the temporal lobe and their interactions.

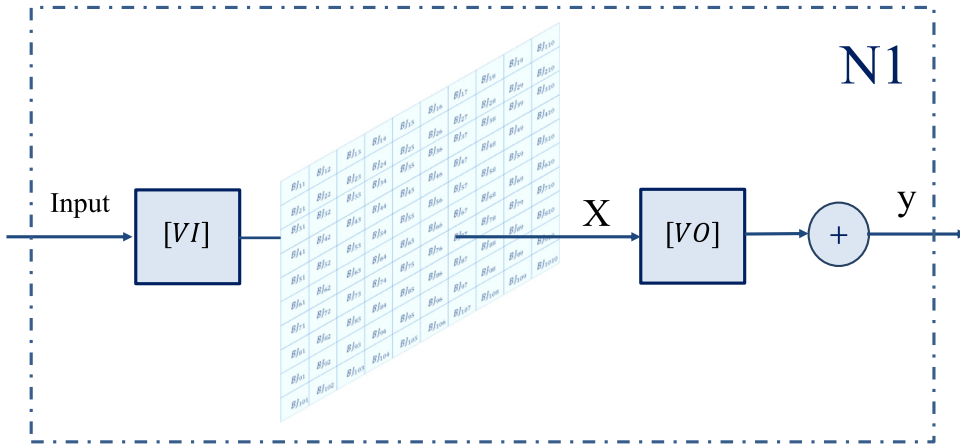


Fig. 3. The first part of the model (N_1), which is a 2D square domain consisting of 10×10 grid points. As it represented, X is made by multiplying the input to the input weights and passing through Bj 's Functions and GCM coupling. Finally aggregate of X which is multiplies to the output weights; make the y as an output of the N_1 .

magnetic fields [46]. Structure of these neural networks have major role in controlling the activity of the brain, and epileptic behaviors can be linked to that [47].

Clinical signs of epileptic seizure go from consciousness, sensory-motor and psychological symptoms (such as nausea and seeing aura) to more well-known symptoms such as excessive activity of neurons and muscle tremors. The variety in symptoms related to the onset of seizures makes the diagnosis of epilepsy not an easy task. The research evidences suggest that there is rather significant energy generated during epileptic activities. As it illustrated in Fig. 1, this enormous energy can be detected in EEG recording as a harmonious pattern with higher than usual amplitude. One of the probable explanations of these synchronize high-amplitude signals is the synergic activity of a group of neurons synchronously firing with each other.

The only effective and available treatment method for controlling epilepsy is to use medicine. However, in many cases it fails to control the seizures or even reduce its side effects such as the lack of coordination in walking, welding, aplastic anemia, or liver infection. In some severe cases, the best option is electrical stimulation through invasive brain surgery.

3. The proposed model

In this section, we introduce a novel map-based model of the temporal lobe epilepsy. The proposed model is a combination of an analytic model and a mass model (Fig. 2). The model has two main parts, N_1 and N_2 , representing different portions of the temporal lobe and their interactions. The first part N_1 contains a 2D square domain consisting of 10×10 grid points. Each grid point is a neural network originally developed by Baghdadi [10]. Let's call each of them by Bj , that are indeed represent different parts of the temporal lobe which are linked to each other based on a network structure. Synaptic connection between nodes i and j are modeled by VI_{ij} and VO_{ij} weights which VI_{ij} models the input weights and VO_{ij} indicates the out put weights. We use Global Coupled Methed (GCM) as a coupling method and a no-flux boundary condition is applied. Total output of each Bj with different synaptic weights in N_1 , is fed to N_2 to produce the overall activity (Fig. 3).

The output of N_1 is obtained as:

$$X_{ij} = (1 - \varepsilon)Bj(k \times z \times VI_{ij}) + \frac{\varepsilon}{4} [Bj(k \times z \times VI_{ij-1}) + Bj(k \times z \times VI_{ij+1}) + Bj(k \times z \times VI_{i-1j}) + f(k \times z \times VI_{i+1j})] \quad (1)$$

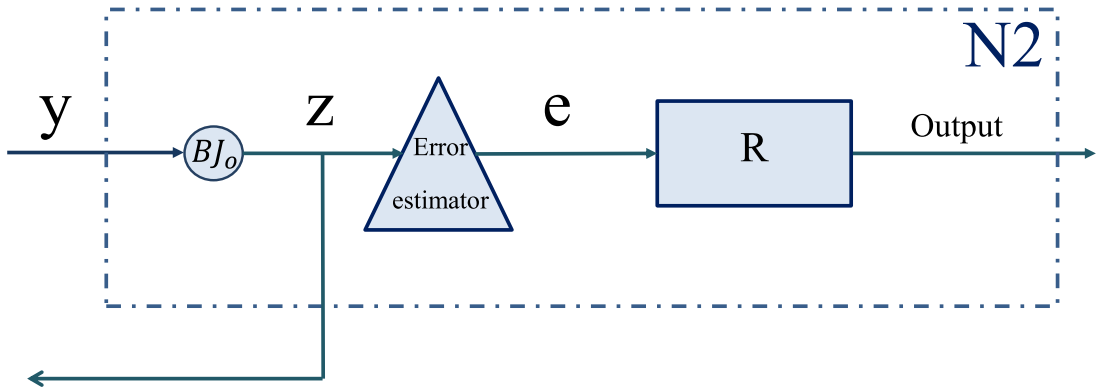


Fig. 4. The second part of the model (N_2), which represents the interaction in neural networks. This part includes three steps, first, y which is the output of previous part is returned to the model workspace by passing through a BJ , the output of this part is named Z . Then a block of error estimator determine the nature of activity which can be periodic or chaotic (e). Finally, the output of the model is produced by a block of Rulkov neural model.

$$y = \sum_{j=1}^{N=10} \sum_{i=1}^{N=10} VO_{ij} \times X_{ij} \quad (2)$$

which is a linear plane of N coupled BJ maps, with nearest neighbor diffusive coupling and periodic boundary conditions, $\varepsilon = 0.1$ represents the coupling parameter and $k = 1$ is a feedback gain. Since the cascading of the process make it confusing, we use the virtual variables such as X , y and z to explain the procedure. X is made by multiplying the input to the input weights and passing through BJ 's Functions and coupling procedure. Finally aggregate of each X which is multiplies to the output weights; make the y as an output of the N_1 .

Each BJ is a multilayer perceptron (MLP) artificial neural network (ANN), which is formed by interaction of two important parts of the inhibitory and excitatory synaptic activity. The input is first multiplied by the initial weights, and is then fed into two activation functions which are considered to be hyperbolic tangent function in this work. The first part contributes to the output of the model with a positive sign, which models the excitation force and the second part negatively contributes to the output of the model to model the inhibition. BJ model is described as

$$BJ : out(n+1) = B \times \tanh(w_1 \times out(n)) - A \times \tanh(w_2 \times out(n)) \quad (2)$$

As it has been shown in [10], all coefficients of BJ model including A , B , w_1 , w_2 represent the weights of the synapses' which are regulated by the release of different neurotransmitters. Therefore, it can be considered that the values of A might be correlated with the amount of inhibitory or GABA neurotransmitter and the values of B can be associated with the amount of excitatory or Glutamate neurotransmitter.

The second major part of the proposed model is N_2 , which represents the interactions in the neural network. This part is a black box modeling of the brain activities which are recorded by EEG. Fig. 6 is a graphical illustration of N_2 .

The output of N_1 (y), which represents the overall activities of the different part of N_1 is fed into the second part (N_2). For the first step, a BJ model with parameters as A_0 , B_0 , and w_0 is considered to return the output "y" to the model's workspace, after which the box of error estimator determines the dominant activity of N_1 (excitatory or inhibitory). The output of error estimator "e" acts as an activation signal for the main part R , which is considered to be Rulkov neuron model. The mathematical equations of the output are as follows (Fig. 4).

$$z = B_0 \times \tanh(w_0 \times y) - A_0 \times \tanh(w_0 \times y) \quad (3)$$

$$e = y(n-p) - y(n) \quad (4)$$

An error signal is provided by the absolute differences between the current sample and p -th sample. By searching the parameter space (p), one can determine whether the signal is periodic. Indeed, "e" determines the dominant activity in N_1 .

$$out(n+1) = (1.1 - M(e))u(n) \quad (5)$$

where $M()$ is a Hyperbolic tangent sigmoid transfer function (refer to Eq. (10)) and $u(n)$ is determined by the slow variable in Rulkov equation at the time instance of n , as follows:

$$R : \begin{cases} v(n+1) = (1 - Y(u(n))) \times f(v(n), v(n-1), k) + \varepsilon(u(n))v_p \\ u(n+1) = \begin{cases} u_s & v(n) > 0 \text{ or } v(n-1) > 0 \\ (1 - \mu)u(n) - g \times u(n)(1 - u(n))^2 & \text{other} \end{cases} \end{cases} \quad (6)$$

BJ_{11}	BJ_{12}	BJ_{13}	BJ_{14}	BJ_{15}	BJ_{16}	BJ_{17}	BJ_{18}	BJ_{19}	BJ_{110}
BJ_{21}	BJ_{22}	BJ_{23}	BJ_{24}	BJ_{25}	BJ_{26}	BJ_{27}	BJ_{28}	BJ_{29}	BJ_{210}
BJ_{31}	BJ_{32}	BJ_{33}	BJ_{34}	BJ_{35}	BJ_{36}	BJ_{37}	BJ_{38}	BJ_{39}	BJ_{310}
BJ_{41}	BJ_{42}	BJ_{43}	BJ_{44}	BJ_{45}	BJ_{46}	BJ_{47}	BJ_{48}	BJ_{49}	BJ_{410}
BJ_{51}	BJ_{52}	BJ_{53}	BJ_{54}	BJ_{55}	BJ_{56}	BJ_{57}	BJ_{58}	BJ_{59}	BJ_{510}
BJ_{61}	BJ_{62}	BJ_{63}	BJ_{64}	BJ_{65}	BJ_{66}	BJ_{67}	BJ_{68}	BJ_{69}	BJ_{610}
BJ_{71}	BJ_{72}	BJ_{73}	BJ_{74}	BJ_{75}	BJ_{76}	BJ_{77}	BJ_{78}	BJ_{79}	BJ_{710}
BJ_{81}	BJ_{82}	BJ_{83}	BJ_{84}	BJ_{85}	BJ_{86}	BJ_{87}	BJ_{88}	BJ_{89}	BJ_{810}
BJ_{91}	BJ_{92}	BJ_{93}	BJ_{94}	BJ_{95}	BJ_{96}	BJ_{97}	BJ_{98}	BJ_{99}	BJ_{910}
BJ_{101}	BJ_{102}	BJ_{103}	BJ_{104}	BJ_{105}	BJ_{106}	BJ_{107}	BJ_{108}	BJ_{109}	BJ_{1010}

Fig. 5. The 2×6 square of BJs as the foci which is shown by the different color.

It should be noted that γ is a Heaviside function and x_{th} is an adjustable threshold.

$$\varepsilon(x - x_{th}) = \begin{cases} 1 & x \geq x_{th} \\ -1 & x < x_{th} \end{cases} \quad (7)$$

The nonlinear function $f(v(n), v(n-1), k)$ is as follows:

$$f(v(n), v(n-1), k) = \begin{cases} \frac{\alpha}{1-v(n)} + k & v(n) \leq 0 \\ 3.2 + k & 0 < v(n) < 3.2 + u \text{ and } v(n-1) \leq 0 \\ -1 & 3.2 + u \leq v(n) \text{ or } v(n-1) > 0 \end{cases} \quad (8)$$

$$g = g_{opt} + D(e) \quad (9)$$

$$M(x) = D(x) = \tanh(x) \quad (10)$$

where $k = \beta + I_{ext}$ is a linear combination of an internal and external trigger. Parameter μ is responsible for the duty time of the pulse and the other control parameter g determines the form of generated pulse at the edge of the transition from high to low. u_s in Eq. (6) controls the location of the starting point [49].

4. Results and discussion

As it mentioned before, foci is an area where the seizure usually initiates. One of the most common causes of seizure onset is the lack of correct information processing in foci. Imbalance of inhibitory and excitatory forces may disturb the normal process of the brain activity and initiate the seizures [41,42]. The major mechanism behind the proposed model in this work is to make a balance between inhibitory and excitatory activities, which is performed by changing the excitatory and inhibitory forces. The first step is to consider one part of the model as foci, from which a partial seizure starts. We then study the parameter space of the inhibitory or excitatory coefficients by setting it as the bifurcation parameter (A or B), while the other parameters are fixed. Indeed, by doing so we assume that the only abnormality causing the disease is related to the inhibitory and excitatory parameters, while other parameters are in normal ranges. This way, only some of the BJs are considered to be malfunctioning in order to play the role of foci. Here, we set 2×6 square of BJs as the foci (as shown in a different color represented by Fig. 5) and study the bifurcation diagram with respect to the parameter A_s . Thus according to the underlying physiological mechanisms, the synchronous hyperactive behavior should start to propagate from the foci to the other parts of the network and adversely affect the normal overall activity.

It is worth to mention that our aim here is not to model the exact and real physiological value of the parameters. It is instead to try to represent the sensitivity of the model to the parameter value whenever the brain loses its control in adjusting them. Sometimes, the behavior of a system can completely switch to an undesired one with only small changes in the parameter value. All the parameters in their normal range are given in Tables 1–3.

Fig. 6 represents the bifurcation diagram of the proposed model for different values of A_s , which is a representative parameter for the inhibitory forces of foci when the rest of the parameters have normal values. For investigating the behavior of the system by changing the excitatory forces in foci, the bifurcation diagram of the system for different values of B_s is plotted in Fig. 7. The rest of the parameters are set to their normal value. For a better view, enlarged bifurcation views with two example time series is shown in Figs. 8 and 9.

Table 1
The values for the parameter in their normal range.

Parameter	Value	Parameter	Value
A_{ij}	8.345	v_p	-0.8
B_{ij}	5.821	u_s	1.3
w_{1ij}	1.487	x_{th}	0.01
w_{2ij}	0.2223	μ	0.07
k	1	α	3.2
a_1	0.1.	β	5.9
a_2	1	g_{opt}	0.3

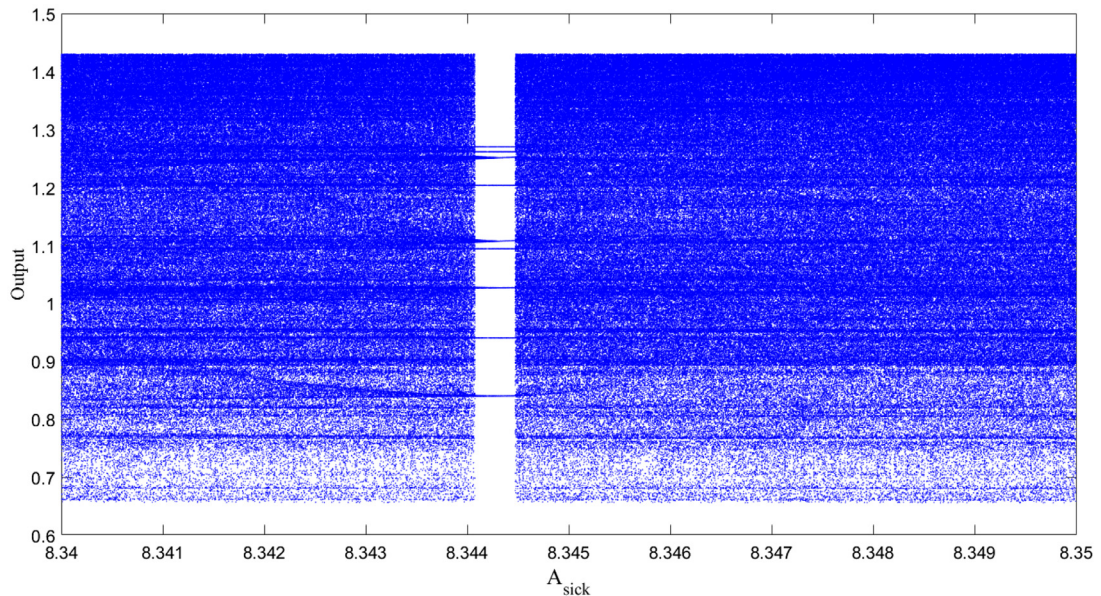


Fig. 6. Bifurcation diagram of the proposed model for different values of A_s (the inhibitory parameter of the foci), while other parameters are set at their normal values.

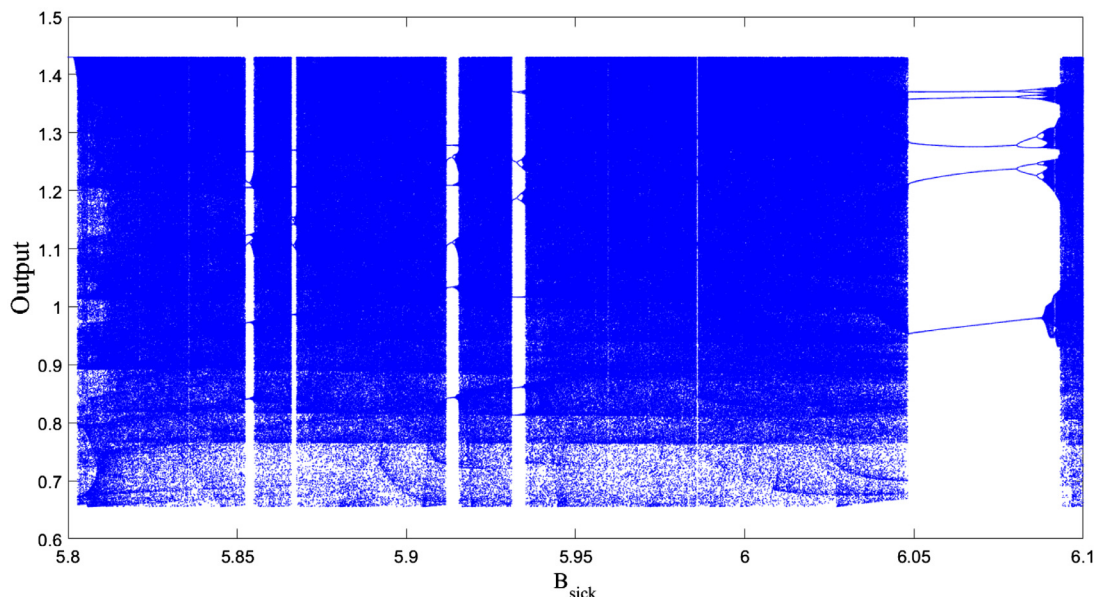


Fig. 7. Bifurcation diagram of the proposed model for different values of B_s (the excitatory parameter of the foci), while other parameters are set at their normal values.

Table 2The matrix of $VI_{10 \times 10}$.

$VI_{11} = 0.5129$	$VI_{12} = 0.2287$	$VI_{13} = 1.0323$	$VI_{14} = 0.5127$	$VI_{15} = 1.8071$	$VI_{16} = 0.6606$	$VI_{17} = 0.3606$	$VI_{18} = 0.9443$	$VI_{19} = -0.7904$	$VI_{110} = -0.8138$
$VI_{21} = 0.6646$	$VI_{22} = -0.5248$	$VI_{23} = -0.1457$	$VI_{24} = -0.9221$	$VI_{25} = 1.3242$	$VI_{26} = -0.3403$	$VI_{27} = -1.2679$	$VI_{28} = 1.0107$	$VI_{29} = 0.9380$	$VI_{210} = -0.2081$
$VI_{31} = -0.8177$	$VI_{32} = -0.0869$	$VI_{33} = 0.5942$	$VI_{34} = 0.6603$	$VI_{35} = -0.8566$	$VI_{36} = 0.5842$	$VI_{37} = -0.1240$	$VI_{38} = -0.2638$	$VI_{39} = -1.1459$	$VI_{310} = 0.1409$
$VI_{41} = 0.0320$	$VI_{42} = -1.9483$	$VI_{43} = 0.4101$	$VI_{44} = 0.3483$	$VI_{45} = -0.6664$	$VI_{46} = -0.8489$	$VI_{47} = 0.6055$	$VI_{48} = -1.2009$	$VI_{49} = 0.8039$	$VI_{410} = 0.2162$
$VI_{51} = 0.1433$	$VI_{52} = 0.8196$	$VI_{53} = -2.1895$	$VI_{54} = 0.9495$	$VI_{55} = -0.2162$	$VI_{56} = -0.7768$	$VI_{57} = -0.4411$	$VI_{58} = 0.4499$	$VI_{59} = -1.4127$	$VI_{510} = -1.5075$
$VI_{61} = 0.1352$	$VI_{62} = 1.5002$	$VI_{63} = 0.5586$	$VI_{64} = -0.8390$	$VI_{65} = -0.5099$	$VI_{66} = -0.4422$	$VI_{67} = -0.6993$	$VI_{68} = -0.3294$	$VI_{69} = -0.8209$	$VI_{610} = -1.5572$
$VI_{71} = -0.3124$	$VI_{72} = 1.1065$	$VI_{73} = -0.6354$	$VI_{74} = -0.7391$	$VI_{75} = 1.1318$	$VI_{76} = -0.1153$	$VI_{77} = 0.5991$	$VI_{78} = 1.4647$	$VI_{79} = 0.3639$	$VI_{710} = 0.0153$
$VI_{81} = 0.2529$	$VI_{82} = -0.4546$	$VI_{83} = 0.1700$	$VI_{84} = -1.0591$	$VI_{85} = -0.6569$	$VI_{86} = 1.0526$	$VI_{87} = -0.4960$	$VI_{88} = 0.7468$	$VI_{89} = -1.1429$	$VI_{810} = -0.0523$
$VI_{91} = 0.5805$	$VI_{92} = 1.1201$	$VI_{93} = -0.7950$	$VI_{94} = -0.6473$	$VI_{95} = 0.3949$	$VI_{96} = 0.2537$	$VI_{95} = -0.1067$	$VI_{98} = -0.8487$	$VI_{99} = 1.1556$	$VI_{910} = -2.4317$
$VI_{101} = 0.0525$	$VI_{102} = -0.1850$	$VI_{103} = 1.8261$	$VI_{104} = 0.8585$	$VI_{105} = -0.1906$	$VI_{106} = 0.1846$	$VI_{105} = -0.1906$	$VI_{108} = -0.5381$	$VI_{109} = 1.0097$	$VI_{1010} = -0.3677$

Table 3The matrix of $VO_{10 \times 10}$.

$VO_{11} = 0.1706$	$VO_{12} = -0.6952$	$VO_{13} = 0.1525$	$VO_{14} = -0.4455$	$VO_{15} = -0.3482$	$VO_{16} = 0.0862$	$VO_{17} = 0.8091$	$VO_{18} = 0.5597$	$VO_{19} = 0.2748$	$VO_{110} = -0.6824$
$VO_{21} = -0.4871$	$VO_{22} = -0.1336$	$VO_{23} = -0.1241$	$VO_{24} = 0.2129$	$VO_{25} = 0.2160$	$VO_{26} = 0.0008$	$VO_{27} = -0.35$	$VO_{28} = -0.4246$	$VO_{29} = -0.0654$	$VO_{210} = 0.7954$
$VO_{31} = 0.7114$	$VO_{32} = 0.6636$	$VO_{33} = -0.6733$	$VO_{34} = 0.1162$	$VO_{35} = 0.0116$	$VO_{36} = 0.2440$	$VO_{37} = 1.0253$	$VO_{38} = 0.2418$	$VO_{39} = 0.5023$	$VO_{310} = -0.0466$
$VO_{41} = -0.3701$	$VO_{42} = -0.1917$	$VO_{43} = 0.1804$	$VO_{44} = 0.9447$	$VO_{45} = -0.5240$	$VO_{46} = -0.0594$	$VO_{47} = -0.5553$	$VO_{48} = -1.1447$	$VO_{49} = -0.1394$	$VO_{410} = -0.4383$
$VO_{51} = 0.0991$	$VO_{52} = -0.6543$	$VO_{53} = 0.4867$	$VO_{54} = 0.5828$	$VO_{55} = 0.4026$	$VO_{56} = 0.5424$	$VO_{57} = 0.0909.$	$VO_{58} = -1.1599.$	$VO_{59} = -0.1213$	$VO_{510} = 0.3390$
$VO_{61} = -0.0830$	$VO_{62} = 0.2484$	$VO_{63} = -0.2729$	$VO_{64} = -0.2998$	$VO_{65} = 0.3302$	$VO_{66} = 0.98876$	$VO_{67} = 0.4158$	$VO_{68} = -0.1919$	$VO_{69} = -0.9812$	$VO_{610} = 0.9252$
$VO_{71} = -0.1415$	$VO_{72} = 0.1371$	$VO_{73} = 0.5865$	$VO_{74} = 0.5259$	$VO_{75} = 0.0458$	$VO_{76} = 0.3175$	$VO_{77} = 0.9448$	$VO_{78} = 0.2141$	$VO_{79} = 0.1149$	$VO_{710} = 0.1369$
$VO_{81} = 0.4007$	$VO_{82} = -0.5664$	$VO_{83} = 0.6025$	$VO_{84} = 0.1480$	$VO_{85} = 0.5470$	$VO_{86} = 0.0354$	$VO_{87} = -0.8093$	$VO_{88} = -0.0592$	$VO_{89} = -0.1178$	$VO_{810} = -0.3648$
$VO_{91} = 0.2637$	$VO_{92} = 8578$	$VO_{93} = -0.4563$	$VO_{94} = -0.5964$	$VO_{95} = -0.4540$	$VO_{96} = 0.7816$	$VO_{97} = 0.0339$	$VO_{98} = 1.0637$	$VO_{99} = 0.2814$	$VO_{910} = 0.1893$
$VO_{101} = -0.1439$	$VO_{102} = 0.1582$	$VO_{103} = 0.1951$	$VO_{104} = 0.0199$	$VO_{105} = -0.2998$	$VO_{106} = -0.4069$	$VO_{107} = 0.7217$	$VO_{108} = 0.0767$	$VO_{109} = -1.0247$	$VO_{1010} = -0.0593$

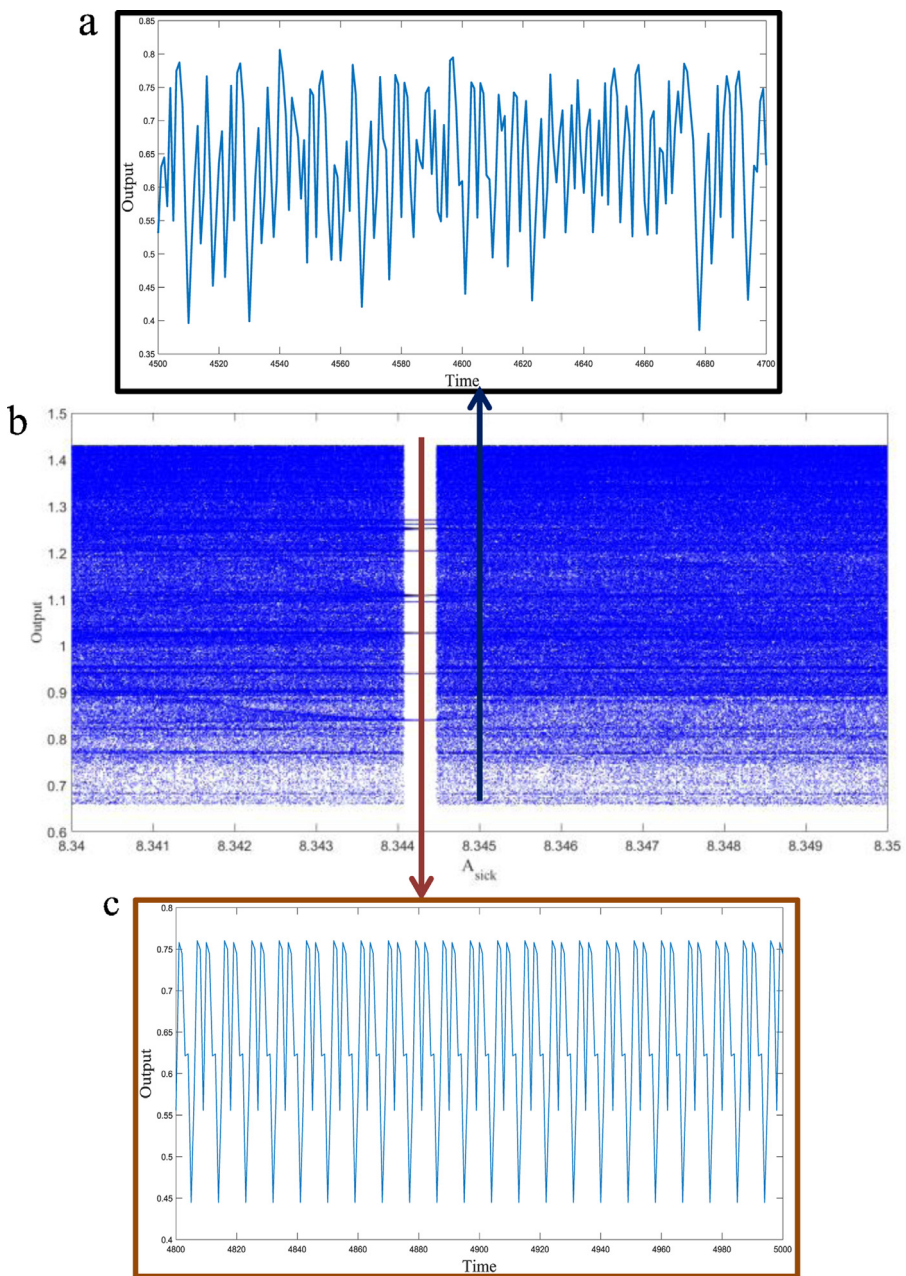


Fig. 8. The enlarged plot of Fig. 7 with two sample time series of the proposed system, the normal range of parameter A (A_{normal}) and A_s ($A_{\text{normal}} = 8.345$, $A_s = 8.3443$).

It is clear from Figs. 8 and 9 that there are some periodic windows in the midst of chaos. Thus, the chaotic behavior of the system can be changed to periodic behavior by a slight change in the bifurcation parameter. For example, if the parameter A in Fig. 8 changes from 8.345 to 8.3443 or parameter B in Fig. 9 changes from 5.821 to 5.853, the chaotic behavior of the model suddenly changes to a periodic behavior. By analyzing the bifurcation diagram for parameter A (neurotransmitter GABA) and B (neurotransmitter Glutamate), it can be found that the model is able to produce complex behaviors. However, we need to further check the behavior of produced time series by changing these parameters. Fig. 11 shows how changing parameter A and B affects them.

As mentioned in previous sections, if the balance of the excitatory and inhibitory neurotransmitter weakens, the system behavior goes to the synchronous mood and seizure start to happen. Having a possibility of restoring the system into the

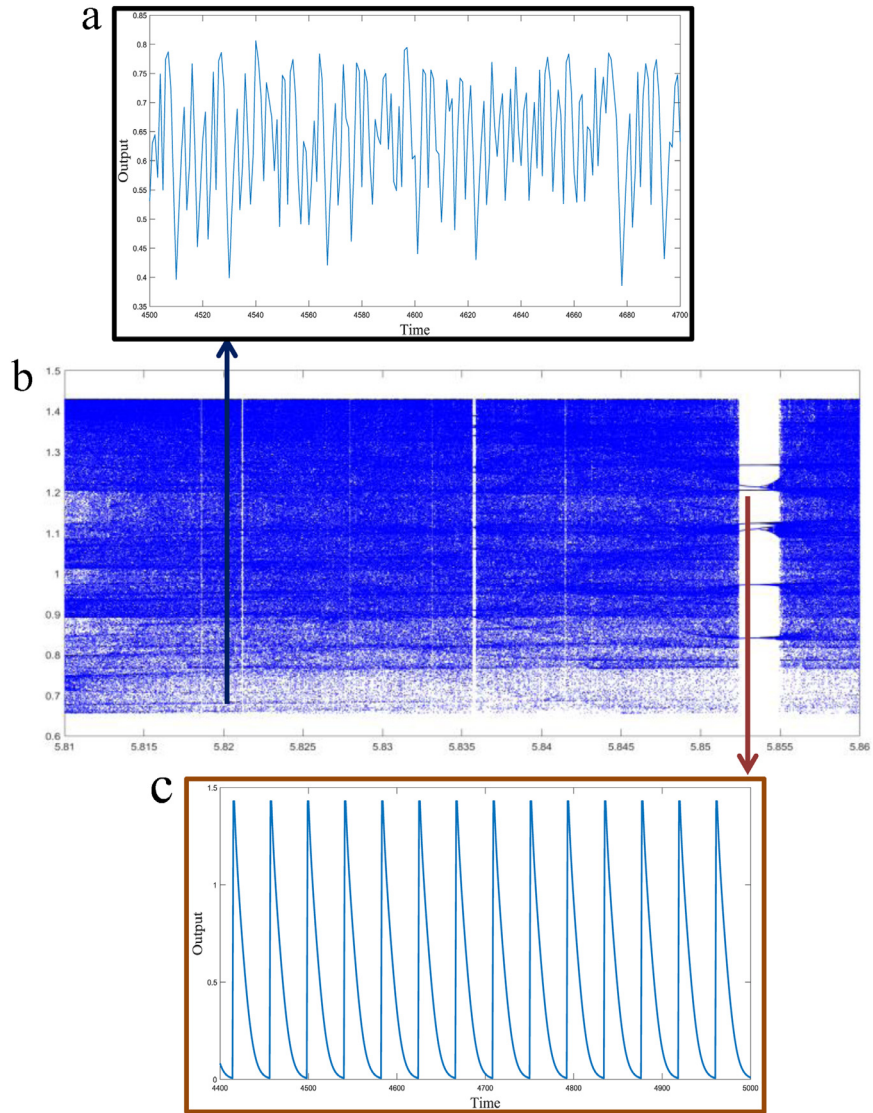


Fig. 9. The enlarged plot of Fig. 8 with two sample time series of proposed system, the normal range of parameter B (B_{normal}) and B_s ($B_{\text{normal}} = 5.821$, $B_s = 5.853$).

normal state without changing the parameters and by only including treatments, would be a step forward in the treatment and control of the seizure. All the simulations above are performed by setting the feedback gain as $k=1$. We further investigate the behavior of the system by changing the feedback gain as a bifurcation parameter, and the results are shown in Fig. 11. It is clear that by changing the value of the feedback gain one can efficiently control the behavior of the system. If a treatment such as electrical stimulation is applied to influence the interactions of different part of the system (N_1 and N_2), one might be able to restore the overall behavior of the model to the normal state without changing the value of its parameters. Fig. 12 shows how a slight change in the value of the feedback gain can restore the chaotic behavior of the model and change the abnormal periodic mood to a normal one. Thus, an important direction for future studies in this field could be to find effective strategies to optimally influence the brain interactions in a way to control the seizures.

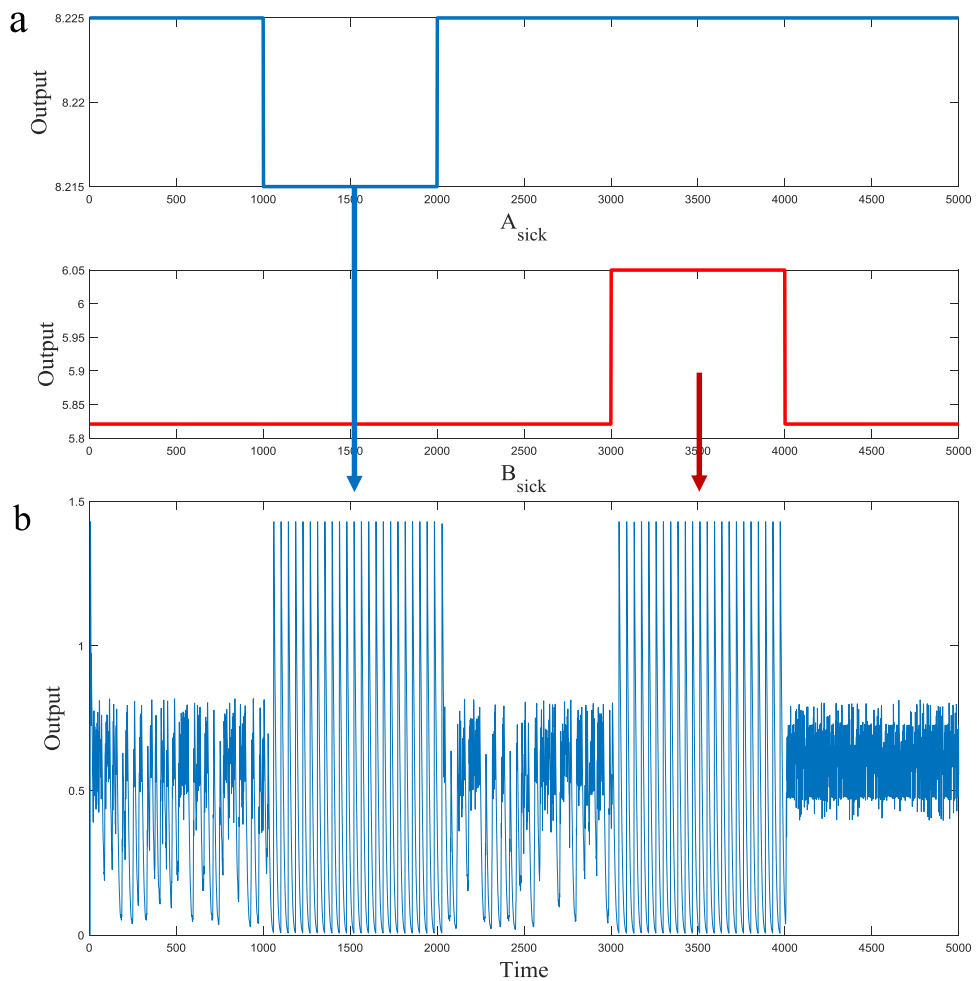


Fig. 10. Time series of the system when the parameter A_s (Blue one) and B_s (Red one) change. For interpretation of the references to color in this figure legend, the reader is referred to the web version of this article.)

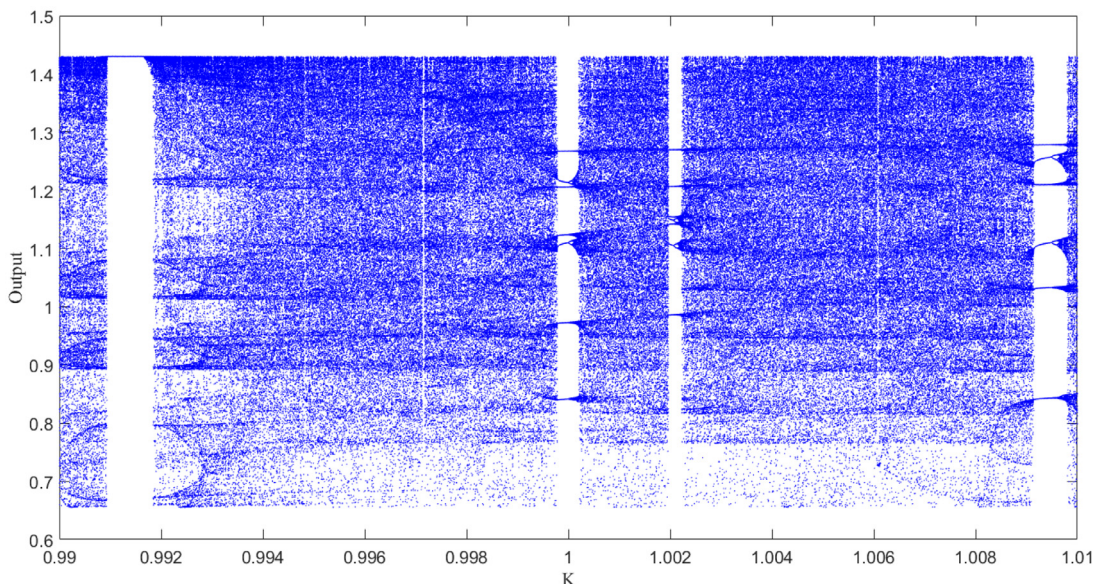


Fig. 11. Bifurcation diagram of the system when the feedback gain is changed as a bifurcation parameter.

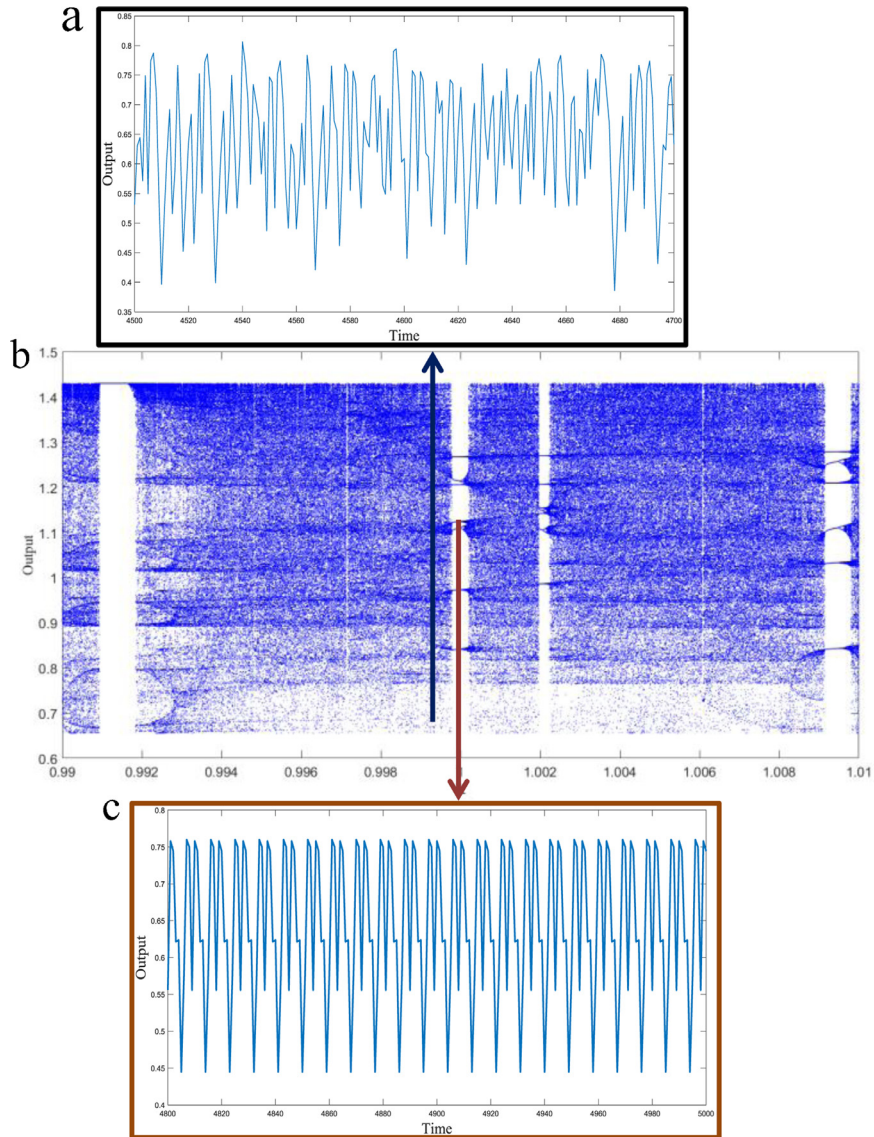


Fig. 12. The enlarged plot of Fig. 11 with two sample time series of the proposed model. As it is represented the slight changes in the value of the feedback gain can change the overall behavior of the system.

5. Conclusions

Epilepsy is the second most common neurological disorder characterized by seizure. It can be effectively diagnosed by visually observing the EEG recorded from the brain. Among different types of epilepsy, temporal lobe epilepsy is the most common type accounting for about one-third of the cases. This paper proposed a mathematical model to study the temporal lobe epilepsy. Normal behavior of the brain under the proposed model is when it shows a chaotic behavior, whereas its periodic behavior indicates an abnormal epileptic behavior. We carried out extensive numerical simulations and studied bifurcation diagrams of the control parameters. Our proposed method includes feedback gain, as effective control parameters, by which one can control the behavior of the model and change its abnormal periodic behavior to normal chaotic behavior. This model provides a useful mathematical tool to get further insights on the mechanisms underlying the epileptic seizures.

Acknowledgment

Sajad Jafari and Shirin Panahi were supported by Iran National Science Foundation (No. 96000815).

References

- [1] H. Huang, H. Zhou, N. Wang, Recent advances in epilepsy management, *Cell Biochem. Biophys.* 73 (1) (2015) 7–10.
- [2] S.L. Moshé, et al., Epilepsy: new advances, *The Lancet* 385 (9971) (2015) 884–898.
- [3] A.K. Ngugi, et al., Estimation of the burden of active and life-time epilepsy: a meta-analytic approach, *Epilepsia* 51 (5) (2010) 883–890.
- [4] C.C. Jouny, G.K. Bergey, Characterization of early partial seizure onset: frequency, complexity and entropy, *Clin. Neurophysiol.* 123 (4) (2012) 658–669.
- [5] M. de Curtis, M. Avoli, Initiation, propagation, and termination of partial (Focal) seizures, *Cold Spring Harbor Perspect. Med.* 5 (7) (2015) a022368.
- [6] L. Maccotta, et al., Impaired and facilitated functional networks in temporal lobe epilepsy, *NeuroImage: Clin.* 2 (2013) 862–872.
- [7] C. Schmidt, et al., Influence of uncertainties in the material properties of brain tissue on the probabilistic volume of tissue activated, *IEEE Trans. Biomed. Eng.* 60 (5) (2013) 1378–1387.
- [8] Alhawarat, M., T.O. Schepers, and N. Crook, *Investigation of a Chaotic Spiking Neuron Model*. arXiv preprint arXiv:1501.02192, 2015.
- [9] E. Başar, *Chaos in Brain Function: Containing Original Chapters by E. Basar and TH Bullock and Topical Articles Reprinted from the Springer Series in Brain Dynamics*, Springer Science & Business Media, 2012.
- [10] G. Baghdadi, et al., A chaotic model of sustaining attention problem in attention deficit disorder, *Commun. Nonlin. Sci. Numer. Simul.* 20 (1) (2015) 174–185.
- [11] Timofeev, I., et al., *Neuronal Synchronization and Thalamocortical Rhythms in Sleep, Wake and Epilepsy*. 2012.
- [12] R.C. Hilborn, *Chaos and Nonlinear Dynamics: An Introduction for Scientists and Engineers*, Oxford University Press, Oxford, 2000.
- [13] M. Karsai, et al., Universal features of correlated bursty behaviour, *Sci. Rep.* 2 (2012) 397.
- [14] L. Lasemidis, J. Sackellares, Chaos theory and epilepsy, *The Neuroscientist* 2 (1996) 118–126.
- [15] W.J. Freeman, Simulation of chaotic EEG patterns with a dynamic model of the olfactory system, *Biol. Cybern.* 56 (2–3) (1987) 139–150.
- [16] W.J. Freeman, Strange attractors that govern mammalian brain dynamics shown by trajectories of electroencephalographic(EEG) potential, *IEEE Trans. Circ. Syst.* 35 (7) (1988) 781–783.
- [17] L. Pan, et al., Chaos synchronization between two different fractional-order hyperchaotic systems, *Commun. Nonlin. Sci. Numer. Simul.* 16 (6) (2011) 2628–2640.
- [18] Y. Wang, et al., Dynamics of fractional-order sinusoidally forced simplified Lorenz system and its synchronization, *Eur. Phys. J. Spec. Top.* 223 (8) (2014) 1591–1600.
- [19] S. He, K. Sun, H. Wang, Synchronisation of fractional-order time delayed chaotic systems with ring connection, *Eur. Phys. J. Spec. Top.* 225 (1) (2016) 97–106.
- [20] S. Majhi, M. Perc, D. Ghosh, Chimera states in a multilayer network of coupled and uncoupled neurons, *Chaos: Interdiscip. J. Nonlin. Sci.* 27 (7) (2017) 073109.
- [21] S. Majhi, M. Perc, D. Ghosh, Chimera states in uncoupled neurons induced by a multilayer structure., *Sci. Rep.* 6 (2016) 39033.
- [22] B.K. Bera, et al., Chimera states: effects of different coupling topologies, *Europhys. Lett.* 118 (1) (2017) 10001 (EPL).
- [23] Z. Faghani, et al., Effects of different initial conditions on the emergence of chimera states, *Chaos Solitons Fractals* 114 (2018) 306–311.
- [24] F. Parastesh, et al., Imperfect chimeras in a ring of four-dimensional simplified Lorenz systems, *Chaos Solitons Fractals* 110 (2018) 203–208.
- [25] Z. Rostami, et al., Taking control of initiated propagating wave in a neuronal network using magnetic radiation, *Appl. Math. Comput.* 338 (2018) 141–151.
- [26] Z. Rostami, et al., Wavefront-obstacle interactions and the initiation of reentry in excitable media, *Phys. A: Stat. Mech. Appl.* 509 (2018) 1162–1173.
- [27] B. Ibarz, J.M. Casado, M.A. Sanjuán, Map-based models in neuronal dynamics, *Phys. Rep.* 501 (1) (2011) 1–74.
- [28] M. Lv, J. Ma, Multiple modes of electrical activities in a new neuron model under electromagnetic radiation, *Neurocomputing* 205 (2016) 375–381.
- [29] F. Wendling, et al., Epileptic fast activity can be explained by a model of impaired GABAergic dendritic inhibition, *Eur. J. Neurosci.* 15 (9) (2002) 1499–1508.
- [30] F. Lopes da Silva, et al., Model of brain rhythmic activity, *Biol. Cybern.* 15 (1) (1974) 27–37.
- [31] J. Tang, et al., Delay and diversity-induced synchronization transitions in a small-world neuronal network, *Phys. Rev. E* 83 (4) (2011) 046207.
- [32] Q. Wang, et al., Synchronization transitions on scale-free neuronal networks due to finite information transmission delays, *Phys. Rev. E* 80 (2) (2009) 026206.
- [33] Q. Wang, et al., Synchronization transitions on small-world neuronal networks: effects of information transmission delay and rewiring probability, *Europhys. Lett.* 83 (5) (2008) 50008 (EPL).
- [34] Q. Wang, G. Chen, M. Perc, Synchronous bursts on scale-free neuronal networks with attractive and repulsive coupling, *PLoS One* 6 (1) (2011) e15851.
- [35] Z. Wang, A. Szolnoki, M. Perc, Optimal interdependence between networks for the evolution of cooperation, *Sci. Rep.* 3 (2013) 2470.
- [36] X. Li, R. Rakkiyappan, P. Balasubramaniam, Existence and global stability analysis of equilibrium of fuzzy cellular neural networks with time delay in the leakage term under impulsive perturbations, *J. Frankl. Inst.* 348 (2) (2011) 135–155.
- [37] X. Li, J. Cao, Delay-dependent stability of neural networks of neutral type with time delay in the leakage term, *Nonlinearity* 23 (7) (2010) 1709.
- [38] S.N. Kalitzin, D.N. Velis, F.H.L. da Silva, Stimulation-based anticipation and control of state transitions in the epileptic brain, *Epilepsy Behav.* 17 (3) (2010) 310–323.
- [39] F. Semah, et al., Is the underlying cause of epilepsy a major prognostic factor for recurrence? *Neurology* 51 (5) (1998) 1256–1262.
- [40] A.T. Berg, et al., *Revised terminology and concepts for organization of seizures and epilepsies: report of the ILAE commission on classification and terminology, 2005–2009*, *Epilepsia* 51 (4) (2010) 676–685.
- [41] Miles, R., et al., *Chloride Homeostasis and GABA Signaling in Temporal Lobe Epilepsy*. 2012.
- [42] C. Bernard, Alterations in synaptic function in epilepsy, *Epilepsia* 51 (s5) (2010) 42–42.
- [43] T. Eid, et al., Loss of glutamine synthetase in the human epileptogenic hippocampus: possible mechanism for raised extracellular glutamate in mesial temporal lobe epilepsy, *The Lancet* 363 (9402) (2004) 28–37.
- [44] R.W. Olsen, et al., GABA receptor function and epilepsy, *Adv. Neurol.* 79 (1999) 499.
- [45] A. Pitkänen, T.P. Sutula, Is epilepsy a progressive disorder? Prospects for new therapeutic approaches in temporal-lobe epilepsy, *The Lancet Neurol.* 1 (3) (2002) 173–181.
- [46] D. Purves, J.W. Lichtman, *Principles of Neural Development*, Sinauer Associates, Sunderland, MA, 1985.
- [47] Y. Wu, D. Liu, Z. Song, Neuronal networks and energy bursts in epilepsy, *Neuroscience* 287 (2015) 175–186.
- [48] Shoeb, A.H., *Application of Machine Learning to Epileptic Seizure Onset Detection and Treatment*. 2009, Massachusetts Institute of Technology.
- [49] F. Hadaeghi, et al., Toward a complex system understanding of bipolar disorder: A chaotic model of abnormal circadian activity rhythms in euthymic bipolar disorder, *Aust. N. Z. J. Psychiatry* 50 (8) (2016) 783–792.